Research Article

Journal of Environmental Nanotechnology

Biogenic Silver Nanoparticles from *Boerhavia diffusa* L. Against the MCF-7 Breast Cancer Cell Line

V. Karthikeyan, D. Janani, M. Shree Rama and K. Sivakumar*

Department of Biotechnology, Karpaga Vinayaga College of Engineering and Technology, Chengalpattu, TN, India

Received: 09.06.2026 Accepted: 11.07.2026 Published: xx.xx.xxxx

*ksivakumar76@gmail.com

ABSTRACT

Breast cancer is one of the leading causes of cancer-related mortality worldwide, highlighting the need for new, safer, and more effective therapeutic strategies. Phytochemical screening of the *Boerhavia diffusa* L. extract confirmed the presence of flavonoids, phenols, tannins, glycosides, and cardiac glycosides, which may contribute to nanoparticle synthesis and stabilization. UV–Vis spectroscopy confirmed the formation of AgNPs through the appearance of a characteristic surface plasmon resonance peak at 420 nm, while SEM–EDAX, XRD, and FTIR analyses were used for further characterization. SEM revealed predominantly spherical nanoparticles, while XRD confirmed their face-centered cubic crystalline structure. FTIR analysis suggested that phytochemicals from the plant acted as reducing and capping agents. Michigan Cancer Foundation-7 (MCF-7) cell viability was assessed using the 3-(4,5-dimethylthiazol-2-yl)-2,5-diphenyltetrazolium bromide (MTT) assay to evaluate the dose-dependent cytotoxicity of the AgNPs, yielding an IC_{50} value of 36 µg/mL. Apoptosis induction in cells treated with AgNPs was evaluated by morphological observation and staining with acridine orange/ethidium bromide (AO/EtBr) and 4′,6-diamidino-2-phenylindole (DAPI). These results indicate that *B. diffusa*-mediated AgNPs exhibit anticancer activity against MCF-7 cells *in vitro*. Nevertheless, these findings require validation through further *in vivo* and mechanistic studies before the therapeutic potential of the AgNPs can be established.

Keywords: Breast cancer; *Boerhavia diffusa*; Silver nanoparticles; Cytotoxicity.

1. INTRODUCTION

Breast cancer remains a multifaceted global health challenge, necessitating the exploration of novel therapeutic strategies that offer enhanced efficacy and reduced toxicity to healthy cells. Conventional therapeutic approaches, such as surgery, radiotherapy, and chemotherapy, are often effective for localized cancer; however, they are frequently inadequate for managing metastatic cancer (Yeşilot and Dönmez, 2021). The significant side effects and high costs associated with conventional chemotherapy underscore the urgent need for cost-effective and practical cancer therapies (Deivanathan and Prakash, 2023). In this context, nanotechnology has emerged as a promising field because it enables targeted drug delivery systems that minimize systemic toxicity while enhancing therapeutic outcomes in cancer treatment (Agilen *et al.* 2019). Recently, biogenic silver nanoparticles, particularly those synthesized using biological resource extracts, have attracted significant attention for their relative biocompatibility, ease of synthesis, and proven anticancer effects (Firdhouse and Lalitha, 2015; Pandey *et al.* 2025). This emerging field seeks to leverage the unique physical and chemical characteristics of nanoparticles to develop more effective diagnostic tools and cancer therapies (Khan *et al.* 2021).

In recent years, the green synthesis of nanoparticles using plant extracts has provided an economical and environmentally friendly approach, in contrast to traditional chemical methods that utilize toxic reagents and require energy-intensive protocols (Palle *et al.* 2020). Plant-mediated approaches are much more environmentally friendly and offer different biocompatibility and therapeutic potential for evolved synthesis products than chemical approaches, mainly because of the ability of many phytochemicals, such as flavonoids, phenols, tannins, and other bioactive compounds, to act as natural reducing and stabilizing agents (Hamzah, 2026; Hublikar *et al.* 2023). Among metallic nanoparticles, silver nanoparticles (AgNPs) are of particular interest because of their wide range of antimicrobial properties (Balaji and Muthukaliannan, 2016; Firdhouse and Lalitha 2015; Vishal *et al.* 2023). Their unique physicochemical properties, such as high surface area-to-volume ratio, nanosize, and ability to diffuse across biological membranes, can induce cell apoptosis or inhibit vital cellular pathways in cancer cells (Vishal *et al.* 2023). Although advances have been made in conventional cancer therapies, the estimated rise to a projected global incidence of 30 million cases by 2040 (Madhusudanan, 2024) emphasizes the profound need for safer and more targeted therapeutic approaches. This has prompted increasing interest in the plant-mediated

synthesis of metallic nanoparticles, especially AgNPs, as environmentally benign nanomaterials for application in cancer diagnosis and treatment, as well as to overcome the drug resistance and systemic toxicity associated with conventional chemotherapy (Kumarasamy *et al.* 2026; Singh *et al.* 2024; Bharadwaj *et al.* 2021; Todaria *et al.* 2024). In addition, their small size and membrane permeability enable AgNPs to be taken up and accumulated in various cells, making them promising candidates for biomedical applications with clinical potential; however, further studies are required to validate their efficacy and safety (Bharadwaj *et al.* 2021; Halimatussakdiah *et al.* 2025; Todaria *et al.* 2024).

Nonetheless, a deeper investigation is needed into the cytotoxic effects of biogenic AgNPs on the MCF-7 cell line, as well as a comprehensive analysis of these nanoparticles. The green synthesis method leverages the rich phytochemical constituents of plant extracts to facilitate the biological conversion of silver ions (Ag^+) into stable silver nanoparticles (Hosny *et al.* 2025). This method is highly effective because various phytochemical substances, such as flavonoids, terpenoids, and polyphenols, not only serve as reducing agents but also help stabilize the nanoparticles, often providing additional therapeutic benefits. This eco-friendly technique produces nanoparticles with customizable optical, electronic, and catalytic properties, which are essential for a wide range of biomedical applications (Javid and Dilshad, 2023).

This category of biogenic nanoparticles is highlighted due to their demonstrated effectiveness in triggering apoptosis, generating reactive oxygen species, and causing genotoxicity in various cancer cell lines, which has led to their consideration as modern therapeutic agents (Singh *et al.* 2025). Although research on the green synthesis of AgNPs for cancer treatment is on the rise, there remains a substantial gap in fully understanding and characterizing the mechanism of AgNPs derived from medicinal plants such as *Boerhavia diffusa* L. and their cytotoxic effects on human breast cancer cells (Bhandari *et al.* 2022). The understanding of the cytotoxic mechanisms and biomolecular interactions of *B. diffusa* L. extract concerning its anticancer potential against the MCF-7 cell line is incomplete (Bhandari *et al.* 2022), and several studies have reported on plant-derived AgNPs with anticancer properties. This is among the first studies to combine phytochemical screening, four-technique physicochemical characterization (UV–Vis, SEM-EDAX, XRD, FTIR), and multi-assay apoptosis confirmation (MTT, morphology, AO/EtBr, DAPI) specifically for *B. diffusa*-derived AgNPs against MCF-7 cells. This research encompasses the evaluation of various sophisticated staining methods, including, among other aspects, morphological alterations, mitochondrial integrity deterioration, and apoptotic pathways.

2. MATERIALS AND METHODS

2.1 Collection of *Boerhavia diffusa* L. Leaves

Fresh leaves of *B. diffusa* (Fig. 1) were collected from Acharapakkam, Chengalpet, Tamil Nadu, India.

Fig. 1: *Boerhavia diffusa* L. leaves

2.2 Preparation of Aqueous Leaf Extract

The collected *B. diffusa* leaves were washed with distilled water to remove any dust and impurities. 20 g of fresh leaves were boiled in 100 mL of distilled water for 5 min. After boiling, the extract was allowed to cool and was filtered through filter paper (Whatman No. 1). The filtrate was then stored at 4 °C for subsequent experimental use (Iravani, 2011).

2.3 Phytochemical Screening

The phytochemical analysis of the leaf extract was performed using standard protocols (Harborne, 1998) to detect major bioactive constituents.

2.4 Synthesis of Silver Nanoparticles (AgNPs)

Silver nanoparticles were synthesized through an eco-friendly method by adapting an established technique (Ahmed *et al.* 2016). The aqueous leaf extract (10 mL) was added to 90 mL of a 1 mM silver nitrate ($AgNO_3$) solution in triplicate. The mixture was kept in a water bath at 60 °C for 10 min. The synthesized AgNPs were indicated by a color change from pale yellow to dark brown, which is due to surface plasmon resonance. The mixture was centrifuged at 10,000 rpm for 15 min, and the pellet was washed repeatedly with distilled water. The purified nanoparticles were dried at room temperature and stored for further characterization. Nanoparticle yield was calculated gravimetrically as the dry weight of purified AgNPs per 100 mL of reaction volume, expressed in mg/100 mL, with the percentage conversion calculated relative to the $AgNO_3$ input.

2.5 Characterization of Synthesized AgNPs

The reduction of Ag^+ ions and the subsequent formation of AgNPs were monitored using a UV–Vis

spectrophotometer (Shimadzu UV-1800) across a wavelength range of 300–700 nm (Kelly *et al.* 2003). The morphology and nanoparticle size were analyzed using HR-SEM (FEI Quanta FEG 200), and the elemental composition was analyzed by EDAX attached to the SEM instrument (Goldstein *et al.* 2018). The crystalline structure of the AgNPs was characterized using an X-ray diffractometer operating at 45 kV and 30 mA with Cu-Kα radiation, and the diffraction pattern was recorded over a 2θ range of 10–90°. Fourier Transform Infrared (FTIR) spectroscopy (Perkin Elmer Spectrum One) was conducted over the spectral range of 4000–400 cm^{-1} to identify the functional groups in the synthesized nanoparticles (Stuart, 2021).

2.6 *MTT Assay for in vitro Cytotoxicity*

The MTT assay was employed to evaluate the cytotoxicity of the synthesized AgNPs against MCF-7 human breast cancer cells, obtained from the National Center for Cell Science (NCCS) in Pune. The cells were cultured in Dulbecco's Modified Eagle Medium (DMEM) under optimal conditions (37 °C, 5% CO_2) (Mosmann, 1983). A cell density of 1×10^6 cells/mL was seeded into 96-well plates and exposed to varying concentrations of synthesized AgNPs (12.5, 25, 50, and 100 µg/mL) in triplicate for a duration of 24 h. The untreated AgNP cells served as controls. After the incubation period, 10 µL of MTT reagent was added, and the cells were incubated for an additional 4 h. The resulting formazan crystals were dissolved in 100 µL of dimethyl sulfoxide (DMSO), and the absorbance was measured at 570 nm using a microplate reader.

Cell viability was calcula-ted as follows:

$$\text{Cell viability (\%)} = [\text{Mean optical density (OD) of the experimental sample (AgNPs)}/\text{Mean OD value of experimental control}] \times 100$$

The half-maximal inhibitory concentration (IC_{50}) was determined from the dose–response curve.

2.7 Morphological Analysis

MCF-7 cells (1×10^5 cells) were cultured and subsequently treated with AgNPs at the IC_{50} concentration. The cells were fixed with a methanol: acetic acid solution (3:1), mounted on slides, and observed under a phase-contrast inverted microscope (Labomed) to identify morphological alterations (Capes-Davis *et al.* 2021).

2.8 Apoptotic Assays

2.8.1 Acridine Orange/Ethidium Bromide (AO/EtBr) Staining

Cells exposed to the IC_{50} concentration of AgNPs were subsequently fixed and stained using an AO/EtBr (1:1) solution. Following incubation and washing with phosphate-buffered saline (PBS), the cells were observed under a fluorescence microscope (Olympus V1000) at 200× magnification to identify apoptotic changes (Ribble *et al.* 2005).

2.8.2 DAPI Staining

To assess nuclear fragmentation, the treated cells were stained with DAPI at a concentration of 1 µg/mL following fixation. The cells were then incubated in the dark for 20 min and subsequently visualized using a fluorescence microscope (Olympus V1000) at 200× magnification (Kapuscinski, 1995).

2.9 Statistical Analysis

Data are expressed as mean ± SD and were analyzed using one-way ANOVA followed by Tukey's post hoc test (GraphPad Prism); $p < 0.05$ was considered statistically significant.

3. RESULTS AND DISCUSSION

3.1 Phytochemical Analysis

Phytochemical analysis of the aqueous leaf extract of *B. diffusa* revealed the presence of flavonoids, tannins, phenols, glycosides, and cardiac glycosides, while alkaloids, steroids, and saponins were absent (Table 1). These bioactive phytochemicals may contribute to the antioxidant and antimicrobial properties of the extract, with antioxidant activity potentially associated with flavonoids and phenolic –OH groups (Gautam *et al.* 2016; Palle *et al.* 2020). The absence of alkaloids, steroids, and saponins suggests that these phytochemical classes may not contribute significantly to the biological effects of the aqueous extract (Franjić *et al.* 2004).

Table 1. Preliminary phytochemical analysis of the aqueous leaf extract of *B. diffusa*

Phytochemicals	Aqueous extract
Alkaloids	-
Flavonoids	+
Steroids	-
Tannins	+
Saponins	-
Phenols	+
Glycosides	+
Cardiac glycosides	+

Note: + indicates presence; - indicates absence

3.2 Synthesis of Silver Nanoparticles

The aqueous leaf extract of *B. diffusa* without $AgNO_3$ showed no visible change, whereas incubation with $AgNO_3$ resulted in a distinct yellow-to-brown

coloration, indicating the reduction of Ag^{+} ions by phytochemicals in the extract and the formation of AgNPs (Figs. 2a–b). This observation confirmed extracellular bioreduction and nanoparticle synthesis and is consistent with previous findings reporting similar time-dependent activity during the green synthesis of silver nanoparticles using *B. diffusa* leaf extract (Reena and Gayathri, 2024; Kanagavalli *et al.* 2016; Kumarasamy *et al.* 2026; Badi'ah *et al.* 2019; Lee *et al.* 2007).

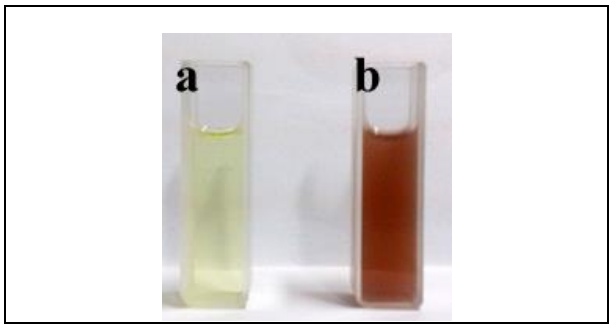

Fig. 2: (a) Aqueous leaf extract and (b) synthesis of AgNPs from leaf extract incubated with $AgNO_3$ solution

3.3 UV–Vis Spectrum of AgNPs Synthesized Using *B. diffusa* Leaf Extract

The UV–Vis spectrum of *B. diffusa*-synthesized AgNPs using leaf extract showed a distinct localized surface plasmon resonance (LSPR) band at approximately 420 nm, confirming the successful formation of Ag nanoparticles. A relatively broad peak indicates a distribution of particle sizes and possible polydispersity (Fig. 3).

The behavior of biogenic AgNPs is strongly linked to the general process where phytochemicals facilitate the reduction that results in nanoparticle creation (Hussain *et al.* 2019; Sangappa *et al.* 2019; Venkataramana *et al.* 2018). Previous research has demonstrated that AgNPs synthesized from various natural extracts exhibit a similar absorption maximum range; differences between 400 and 470 nm represent substantial changes in nanoparticles. This peak broadening is attributed to the polydispersity and heterogeneity in nanoparticle size (Gupta *et al.* 2025; Mariano *et al.* 2018). Consequently, the current spectral findings confirm that *B. diffusa* leaf extract acts as both a reducing and stabilizing agent in forming AgNPs with optical properties akin to those observed in earlier studies (Arulraj *et al.* 2025; Kanagavalli *et al.* 2016). However, the broader LSPR band here indicates a wider size distribution compared to formulations with narrower peaks (Juvé *et al.* 2013).

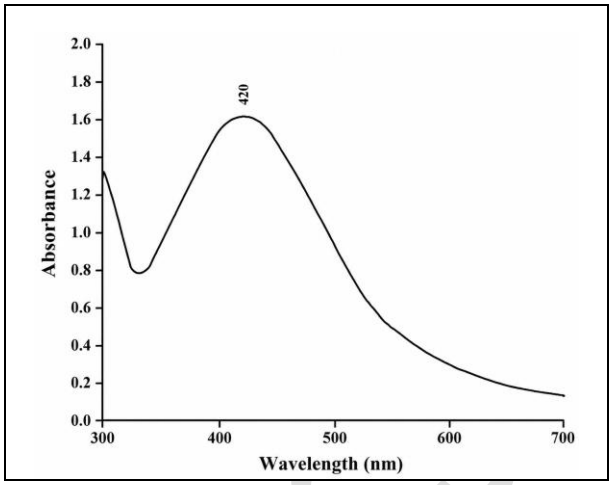

Fig. 3: UV–Vis spectrum of *B. diffusa*-synthesized AgNPs

3.4 SEM and EDAX

The SEM micrograph shows that the synthesized AgNPs are spherical to near-spherical and form a dense, clustered morphology (Fig. 4). The result of SEM analysis revealed that the biosynthesized silver nanoparticles were mainly spherical, with a few agglomerations. The measurement of particle diameters was performed using ImageJ software based on the SEM micrographs. The mean diameter of nanoparticles was 10.47 ± 0.16 nm, with most particles falling between the sizes of 10.3 and 10.7 nm, indicating a narrow particle size distribution. Overall, the image suggests that the leaf extract acts as a capping/stabilizing agent, promoting relatively uniform nanoscale growth and preventing extensive nanoparticle aggregation. In the EDAX spectrum, the characteristic peaks for Ag are clearly visible between 2.98 and 3.35 keV (Table 2), and the same trend was reported by De Leersnyder *et al.* (2020). Additionally, a faint signal for potassium (K) is observed near ~3.3 keV, which is generally attributed to residual inorganic components from the plant extract or minor ions present during synthesis (Wang *et al.* 2013).

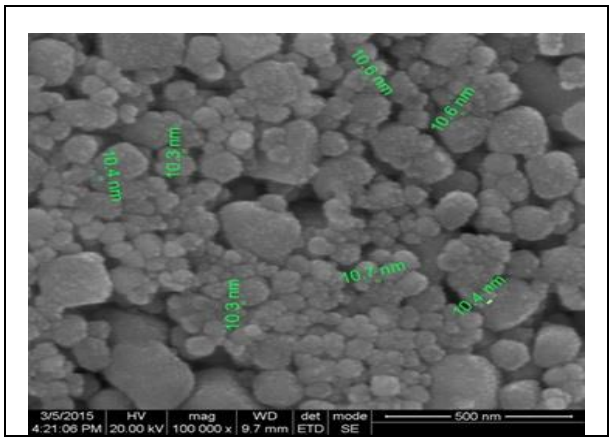

Fig. 4: SEM micrograph of AgNPs synthesized using *B. diffusa* leaf extract

Table 2. EDAX spectral data of AgNPs synthesized using *B. diffusa* leaf extract

Element	Approximate Peak Energy (keV)	X-ray Transition	Observation
Ag	~2.98	Ag Lα	Major characteristic peak confirming elemental silver
Ag	~3.15	Ag Lβ	Characteristic silver peak
Ag	~3.35	Ag Lγ	Minor silver peak

3.5 XRD of AgNPs Synthesized Using *B. diffusa* L. Leaf Extract

The XRD pattern of AgNPs synthesized using *B. diffusa* leaf extract shows diffraction peaks indicating the formation of crystalline silver nanoparticles (Fig. 5). The pattern exhibits a series of characteristic reflections that correspond well to the face-centered cubic (FCC) structure of Ag (metallic Ag). The presence of distinct diffraction peaks confirmed that the AgNPs were crystalline rather than purely amorphous. The main peaks fall in the ~2θ region typical for Ag (FCC), indicating that the nanoparticles were primarily composed of elemental silver (Ag^0). The peak broadening suggests a small crystallite size and/or microstrain, which is common for biosynthesized nanoparticles. The overall peak shape suggests a relatively high degree of nanocrystallinity with some degree of size distribution, which is typical of plant-extract-mediated synthesis. Furthermore, the observed peak positions fall within the characteristic range assigned to FCC silver, aligning with the widely documented lattice assignment of the biosynthesized AgNPs.

The average crystallite size was found to be10–12 nm, confirming the presence of well-crystalline FCC AgNPs mediated by *B. diffusa*. This finding indicates that biomolecules present in the leaf extract governed nucleation, crystal growth, and surface stabilization. These results are consistent with previous reports on AgNP synthesis mediated by plant components (Krishnamoorthy *et al.* 2017; Joy *et al.* 2025; Arulraj *et al.* 2025; Kumarasamy *et al.* 2026).

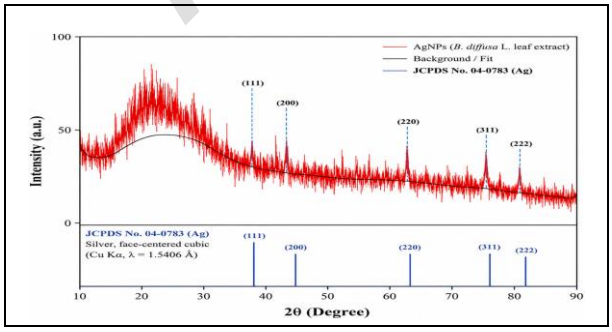

Fig. 5: XRD pattern of *B. diffusa*-synthesized AgNPs

3.6 FTIR of Aqueous Extract and AgNPs Synthesized Using *B. diffusa* Leaf Extract

The FTIR spectra of the aqueous B. diffusa leaf extract (Fig. 6a) and biogenically synthesized AgNPs (Fig. 6b) showed distinct spectral variations following nanoparticle formation, suggesting the involvement of plant phytochemicals in the reduction and stabilization processes. The leaf extract showed the characteristic absorption bands (3412, 2345, 1648 and 618 cm^{-1}) corresponding to O–H/N–H stretching, aliphatic C–H stretching, carbonyl (C=O)/amide vibrations and metal-ligand-associated vibrations, respectively (Table 3). Post AgNP synthesis, these bands shifted to 3390, 2347, 1644 and 762 cm^{-1}, suggesting the involvement of phytochemicals in interacting with the AgNP surface (Table 3).

The overall O–H/N–H stretching band was shifted from 3412 to 3390 cm^{-1}, indicating the involvement of hydroxyl and amino groups of phenolics and proteins in the electron transfer that occurred during the reduction of Ag^+ ions. These functional groups are well known to donate electrons to Ag^+ ions and form an adsorbed layer over the nanoparticle surface, preventing aggregation *via* steric and hydrogen-bond stabilization. The small downshift of the carbonyl/amide band from ~1648 to 1644 cm^{-1} indicates coordination between carbonyl oxygen atoms and surface silver atoms, further establishing flavonoids and proteins, as well as other oxygen-containing metabolites, as efficient capping agents.

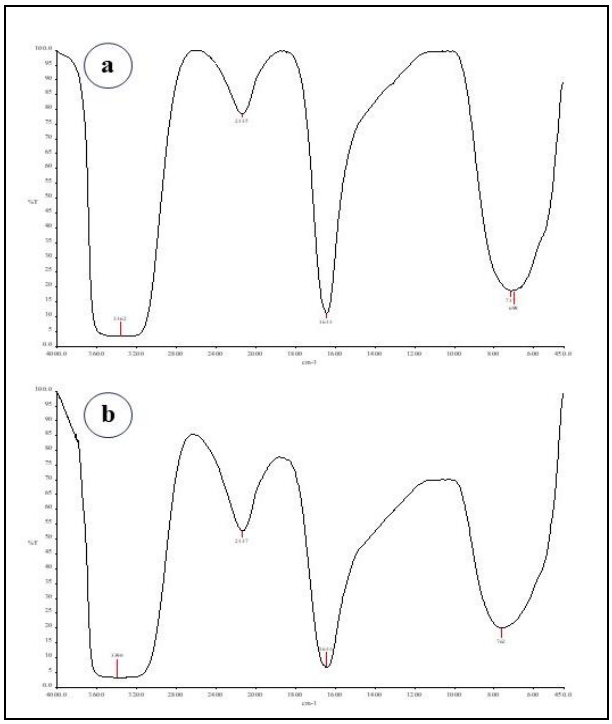

Fig. 6: FTIR spectra of (a) aqueous *B. diffusa* leaf extract and (b) AgNPs synthesized using *B. diffusa* leaf extract

Table 3. FTIR peak assignments of aqueous *B. diffusa* leaf extract and biosynthesized AgNPs

Functional Group	Leaf Extract (cm^{-1})	AgNPs (cm^{-1})	Role in AgNP Synthesis
O–H/N–H stretching	3412	3390	Electron donation for Ag^+ reduction and nanoparticle stabilization through hydrogen bonding
C–H stretching	2345	2347	Indicates the presence of plant-derived organic constituents adsorbed on the nanoparticle surface
C=O / Amide I stretching	1648	1644	Coordination with Ag atoms; reduction of Ag^+ ions and surface capping
Ag–O / Metal–ligand vibrations	618	762	Evidence of Ag–phytochemical interaction and nanoparticle stabilization

The C–H stretching peak showed only a slight shift (2345–2347 cm^{-1}) and remained evident, indicating that organic constituents were retained on the AgNP surface after synthesis. In contrast, the pronounced alteration of the bands in the low-frequency region (618–762 cm^{-1}) indicates the formation of Ag–O or Ag–ligand interactions, suggesting that phytochemicals were chemisorbed onto the nanoparticle surface through covalent interactions rather than physical adsorption.

These shifts, while small for the principal functional groups, are substantial because they flag modifications of the chemical environment after particle formation. The absence of new functional groups and the retention of the main bands indicate that the phytochemicals were not chemically degraded during synthesis but remained attached to the AgNP surface as stabilizing ligands, despite their involvement in redox reactions (Kanagavalli *et al.* 2016; Kumarasamy *et al.* 2026). Similar spectral changes in FTIR spectra have been widely reported for plant-mediated AgNP synthesis, with phenolic compounds, flavonoids, proteins, and other secondary metabolites acting simultaneously as reducing and capping agents, resulting in stable, bioconjugated nanoparticles with good biocompatibility (Aldawsari *et al.* 2026; Kodhaiyolii *et al.* 2019; Krishnamoorthy *et al.* 2017; Gwala Dasi, 2025).

3.7 Assessing *in vitro* Cytotoxicity of AgNPs on MCF-7 Cells

The MTT results indicated a clear, concentration-dependent cytotoxic effect of *B. diffusa*-synthesized AgNPs. Cell viability gradually declined with increasing nanoparticle concentration, showing comparatively higher survival at 12 and 25 µg/mL of 92.30 ± 2.45% and 79.85 ± 2.76%, respectively and marked loss of viability at 50 and 100 µg/mL of 42.35 ± 2.67% and 29.12 ± 2.414%, respectively (Fig. 7). This pattern suggests that the nanoparticles exert dose-dependent antiproliferative activity, consistent with previous findings that AgNPs induce cytotoxicity *via* oxidative stress, mitochondrial dysfunction, and membrane damage. ANOVA followed by Tukey's test showed significant differences in cell viability among the AgNP-treated groups (Fig. 7).

In previous studies on plant-mediated AgNPs, *Boerhavia*-derived nanoparticles have shown potential benefits from phytochemicals that serve as both reducing and capping agents, as well as bioactive components that improve cellular uptake and toxicity (Gericke *et al.* 2024; Mustapha *et al.* 2022; Roy, 2021). The significant reduction in cell viability, with notably high cell death at increased doses, aligns with the existing findings that AgNPs generally exhibit stronger cytotoxicity, which is significantly enhanced by higher NP concentrations. This effect is often linked to factors such as particle size, surface charge, and the type of capping biomolecules (Durán *et al.* 2019; Kim and Ryu, 2013; Zhang *et al.* 2019). The present study offers compelling evidence that *B. diffusa*-synthesized AgNPs are effective cytotoxic agents, comparable to some previously reported plant- and fungus-mediated synthesis methods for AgNPs. Nonetheless, further research is necessary to elucidate the mechanism, selectivity, and safe therapeutic windows of these nanoparticles in mammalian cells, as their anticancer mechanisms remain largely unknown.

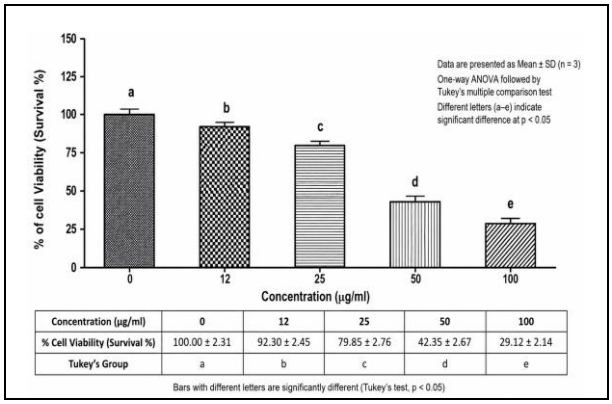

Fig. 7: Cytotoxic activity of *B. diffusa*-synthesized AgNPs. The IC_{50} of AgNPs against MCF-7 cells was 36 µg/mL. Data are expressed as mean ± SD from two experiments.

3.8 Cytomorphological Changes on MCF-7 Cells

The phase-contrast images corroborated the MTT findings, showing that the MCF-7 control cells maintained normal morphology, surface attachment, and cell density. Conversely, AgNP-treated MCF-7 cells at IC_{50} displayed pronounced morphological damage, including reduced confluence,

cell rounding, and partial detachment (Figs. 8a–b). These changes suggest reduced cell viability and disrupted cell–substrate interactions, consistent with nanoparticle-induced cytotoxicity.

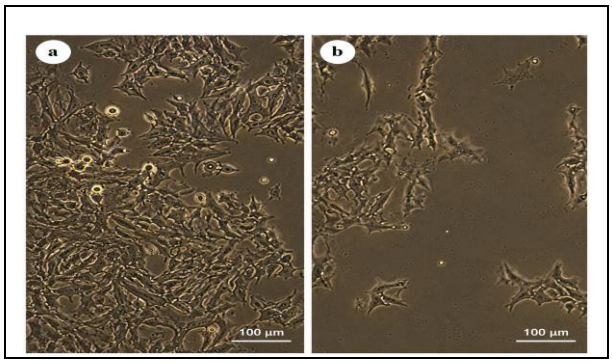

Fig. 8: Phase-contrast images of (a) control cells and (b) AgNP-treated MCF-7 cells at the IC_{50} concentration

3.9 AO-ETBR/DAPI Staining for the Detection of Apoptosis

AO–EtBr staining further validated the cytotoxic effect of *B. diffusa*-synthesized AgNPs on MCF-7 cells. In the control group, the cells predominantly showed green fluorescence, indicating intact membranes and viability. However, upon treatment at the IC_{50}, the appearance of orange/red fluorescence (marked by arrows) suggests increased late apoptosis and/or loss of membrane integrity, consistent with membrane-damage–mediated cell death (Fig. 9).

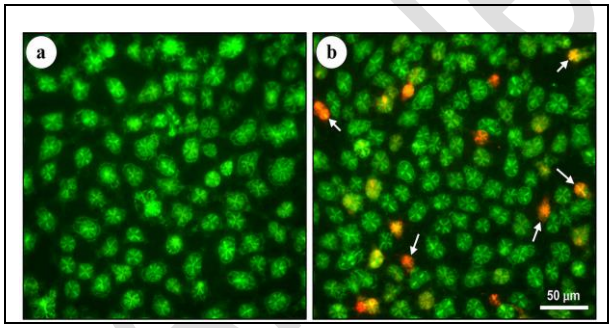

Fig. 9: Fluorescence microscopic images of AO-EtBr-stained control MCF-7 cells (a) and AgNP-treated MCF-7 cells at the IC_{50} concentration (b). Control cells appear green, whereas apoptotic cells appear orange, as indicated by arrows

DAPI staining results supported the cytotoxic effects of *B. diffusa*-synthesized AgNPs on MCF-7 cells. In the control group, the nuclei appeared predominantly smooth and intact (blue fluorescence), indicating normal chromatin organization and viability. In contrast, AgNP-treated cells at IC_{50} exhibited nuclear fragmentation and condensed/irregular nuclear bodies (indicated by arrows), which were characteristic of apoptosis (Fig. 10).

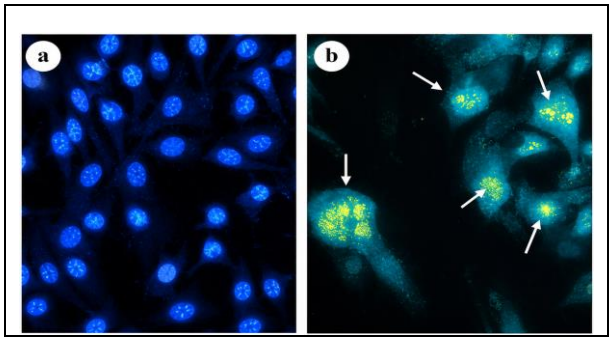

Fig. 10: Fluorescence microscopic images of DAPI-stained (a) control cells and (b) AgNP-treated MCF-7 cells at the IC_{50} concentration. Control cells exhibit intact nuclei, whereas apoptotic cells exhibit fragmented nuclei, as indicated by arrows.

Membrane damage and oxidative stress in the presence of plant-mediated AgNPs can lead to organelle detachment, cytotoxicity, and gradual morphological changes (Tripathi *et al.* 2024). Phase-contrast microscopy showed a gradual progressive decline in normal cell morphology following treatment with AgNPs at the IC_{50} concentration, including cell shrinkage, rounding, loss of adherence, and decreased cell density, indicating cytotoxic injury. Similarly, AO–EtBr dual staining showed a higher proportion of orange/red fluorescent cells compared with the control cells, suggesting loss of membrane integrity associated with apoptosis. DAPI staining further confirmed nuclear condensation and fragmentation or complete nuclear displacement, which are commonly accepted morphological features of apoptosis.

Furthermore, IC_{50}-associated cell rounding and reduced proliferation have been reported in studies of AgNPs against MCF-7 cells, with mitochondrial dysfunction and apoptosis progression described as common pathways (Sangour *et al.* 2021; Ullah *et al.* 2017). The morphological changes observed, together with the decrease in cell viability determined by the MTT assay, suggest that *B. diffusa*-synthesized AgNPs induce apoptotic cell death in a dose-dependent manner. These findings are consistent with previous reports showing that plant-mediated AgNPs induce apoptosis through ROS generation, mitochondrial dysfunction, oxidative stress, and DNA damage (Jabeen *et al.* 2021; Kim and Ryu, 2013; Soni and Gandhi, 2024).

The staining pattern of AO–EtBr obtained in this study is similar to those observed for AgNP-treated MCF-7 cells at IC_{50} concentrations, where viable cells exhibited green fluorescence, whereas apoptotic cells showed orange to red fluorescence due to membrane permeabilization (Durán *et al.* 2019; Zhang *et al.* 2019). Similarly, the chromatin condensation and nuclear fragmentation observed in DAPI-stained nuclei substantiate that the synthesized AgNPs induced an apoptotic response. The results also support the findings

of phase-contrast microscopy and the MTT assay, demonstrating the cytotoxicity of *B. diffusa*-derived AgNPs against MCF-7 cells (Ahmed *et al.* 2016; De Matteis *et al.* 2018; Takáč *et al.* 2023).

While microscopic findings in this study strongly suggest apoptosis, the morphological evidence presented here is largely qualitative. Quantitative determination of the viable, early apoptotic, late apoptotic, and necrotic cell populations was not performed. Further studies with image-based quantification or computer-assisted fluorescence image analysis to determine the percentages of apoptotic and necrotic cells would provide stronger statistical support for the observed morphological changes.

The combined results from phase-contrast microscopy, AO–EtBr staining, DAPI staining, and the MTT assay confirmed that *B. diffusa*-mediated AgNPs induced apoptosis-associated morphological changes in MCF-7 cells at the IC_{50} concentration and provided strong support for their potential as plant-derived anticancer nanomaterials (Iravani, 2011; Jalilzadeh *et al.* 2025).

4. CONCLUSION

In this study, the leaf extract of Boerhavia diffusa L. was employed as a reducing and capping agent for the synthesis of spherical and crystalline silver nanoparticles stabilized by plant-derived phytochemicals. The biosynthesized AgNPs exhibited concentration-dependent cytotoxicity against MCF-7 breast cancer cells and induced characteristic apoptotic morphological and nuclear alterations. These findings suggest that *B. diffusa*-mediated AgNPs have potential as an *in vitro* anticancer agent. However, further studies involving toxicity assessment in normal cell lines, mechanistic investigations of apoptosis, *in vivo* evaluation, and long-term nanoparticle stability are required to establish their safety, efficacy, and potential biomedical applications.

ACKNOWLEDGMENTS

The authors would like to thank the Management, the Principal, and the Department of Biotechnology, Karpaga Vinayaga College of Engineering and Technology, Chengalpattu, TN, India, for providing laboratory facilities for this work.

FUNDING

This research received no specific grant from any funding agency in the public, commercial, or not-for-profit sectors.

CONFLICT OF INTEREST

The authors declare that there is no conflict of interest.

COPYRIGHT

REFERENCES

Agilen, A., Shruthi, P. and Subathra, S., Selective Toxicity of Biosynthesised Silver Nanoparticles on MCF-7 and MDA MB-231 Breast Cancer Cell Lines, *Int. J. Chem. Tech. Res.*, 12(6), 7–16(2019). 10.20902/IJCTR.2019.120602

Ahmed, S., Saifullah, Ahmad, M. Swami, B. L. and Ikram, S., Green synthesis of silver nanoparticles using *Azadirachta indica* aqueous leaf extract, *J. Radiation Res. Appl. Sci.*, 9(1), 1–7, (2016). https://doi.org/10.1016/j.jrras.2015.06.006

Aldawsari, H. M., Ameena, K. Thasneem, C. K., Binmahfouz, L. S., Ashri, L. Y., Ahammed, S. Y. E., and Uoorakkottil, I., Validation, quantification, and molecular docking of isolated eupalitin 3-O-β-D-galactopyranoside in *Boerhavia diffusa* Linn for hepatoprotective and immunomodulatory activity, *Sci. Rep.*, 16, 10578(2026). https://doi.org/10.1038/s41598-026-43266-5

Arulraj, D., Dennis, J., Jegadheeshwari, S., Kesavan, M., and Mistri, T. K., Sustainable L-Cysteine Functionalized Silver Nanoparticles with Dual Biomedical and Catalytic Functions, *Chem. Select*, 10(41), e04869(2025). https://doi.org/10.1002/slct.202504869

Badi'ah, H. I., Seedeh, F., Supriyanto, G. and Zaidan, A. H., Synthesis of Silver Nanoparticles and the Development in Analysis Method, *IOP Conf. Ser.: Earth Environ. Sci.*, 217, 012005 (2019). https://doi.org/10.1088/1755-1315/217/1/012005

Balaji, K. and Muthukaliannan, G. K., Cytotoxic Effect on Cancerous Cell Lines by Biologically Synthesized Silver Nanoparticles, *Brazil. Archiv. Bio. Technol.*, 59, (2016). https://doi.org/10.1590/1678-4324-2016150529

Bhandari, M. M., Raj, S., Kumar, A. and Kaur, D. P., Bibliometric analysis on exploitation of biogenic gold and silver nanoparticles in breast, ovarian and cervical cancer therapy, *Front. Pharmacol.*, 13, 1035769(2022). https://doi.org/10.3389/fphar.2022.1035769

Bharadwaj, K. K., Rabha, B., Pati, S., Sarkar, T., Choudhury, B. K., Barman, A., Bhattacharjya, D., Srivastava, A., Baishya, D., Edinur, H. A., Kari, Z. A., and Noor, N. H. M., Green Synthesis of Gold Nanoparticles Using Plant Extracts as Beneficial Prospect for Cancer Theranostics, *Mol.*, 26(21), 6389 (2021). https://doi.org/10.3390/molecules26216389

Capes-Davis, A. and Freshney, R. I., Freshney's culture of animal cells: a manual of basic technique and specialized applications, *Cells Mol. Bio.,*832(2021).

De Leersnyder, I., Rijckaert, H., De Gelder, L., Van Driessche, I. and Vermeir, P., High Variability in Silver Particle Characteristics, Silver Concentrations, and Production Batches of Commercially Available Products Indicates the Need for a More Rigorous Approach, *Nanomater.*, 10(7), 1394(2020). https://doi.org/10.3390/nano10071394

De Matteis, V., Cascione, M., Toma, C. C. and Leporatti, S., Silver Nanoparticles: Synthetic Routes, In Vitro Toxicity and Theranostic Applications for Cancer Disease, *Nanomater.*, 8(5), 319(2018). https://doi.org/10.3390/nano8050319

Deivanathan, S. K. and Prakash, J. T. J., Biosynthesis of silver nanoparticles from *Rhaphidophora pertusa* leaves extract and its characterization, antimicrobial, anti-oxidant and cytotoxicity activities, *Res. Chem. Intermed.*, 49, 423-439 (2023). https://doi.org/10.1007/s11164-022-04888-2

Durán, N., Rolim, W. R., Durán, M., Fávaro, W. J. and Seabra, A. B., Nanotoxicology of silver nanoparticles: toxicity in aninals and humans, *Quimica Nova*, 42, 206-213(2019). https://doi.org/10.6084/m9.figshare.7941830

Firdhouse, J. and Lalitha, P., Apoptotic efficacy of biogenic silver nanoparticles on human breast cancer MCF-7 cell lines, *Progress Biomater.*, 4, 113–121 (2015). https://doi.org/10.1007/s40204-015-0042-2

Franjić, S., Alkaloids Have a Pronounced Pharmacological Effect, *Pharma Scope Adv. Drug Sci.*, 1(1), (2024). https://doi.org/10.9567/ISSN.2024/WSJ.92

Gautam, P., Panthi, S., Bhandari, P., Shin, J. and Yoo, J. C., Phytochemical Screening and Biological Studies of *Boerhavia diffusa* Linn, *J. Integrat. Nat. Sci.*, 9(1), 72–79(2016). https://doi.org/10.13160/ricns.2016.9.1.72

Gericke, M., Amaral, A. J. R., Budtova, T., De Wever, P., Groth, T., Heinze, T., Höfte, H., Huber, A., Ikkala, O., Kapuśniak, J., Kargl, R., Mano, J. F., Másson, M., Matricardi, P., Medronho, B., Norgren, M., Nypelö, T., Nyström, L., Roig, A., Sauer, M., Schols, H. A., van der Linden, J., Wrodnigg, T. M., Xu, C., Yakubov, G. E., Stana Kleinschek, K. and Fardim, P., The European Polysaccharide Network of Excellence (EPNOE) research roadmap 2040: Advanced strategies for exploiting the vast potential of polysaccharides as renewable bioresources, *Carbohydrate Polym.*, 326, 121633(2024). https://doi.org/10.1016/j.carbpol.2023.121633

Goldstein, J. I., Newbury, D. E., Michael, J. R., Ritchie, N. W. M., Scott, J. H. J. and Joy, D. C., Scanning electron microscopy and X-ray microanalysis, Fourth edition. ed. Springer, New York, NY, U.S.A, (2018).

Gupta, C., Gupta, M. K. and Tripathi, S., Green synthesis of silver nanoparticles using soil bacteria and its antibacterial potential, *J. App. Bio. Biotech.*, 13, 179–186, (2025). https://doi.org/10.7324/jabb.2025.v13.i6.21

Gwala Dasi, D., FTIR-based mapping of biologically active groups in a botanically derived root extract, *Sci. Open Chem.*, (2025). https://doi.org/10.5281/zenodo.17576953

Halimatussakdiah, H., Mardina, V., Amri, Y., Misdi, M., Wahyuningsih, P. and Tan, S. P., Anticancer Efficacy of Silver Nanoparticles Synthesized from Erythrina variegata L. Leaves Extract against A549 Lung Cancer Cell Line, *Sains Malaysiana*, 54(9), 2227–2242 (2025). http://doi.org/10.17576/jsm-2025-5409-10

Hamzah, H., Targeted therapy and biomarker-guided applications of ecofriendly silver nanoparticles in precision oncology, *J. Pharm. Pharmaceu. Sci.*, 28, 15403–15403(2026). http://doi.org/10.3389/jpps.2025.15403

Harborne, J. B., Phytochemical methods: a guide to modern techniques of plant analysis, 3rd ed. ed. Chapman and Hall, London ; New York(1998).

Hosny, S., Gaber, G. A., Ragab, M. S., Ragheb, M. A., Anter, M. and Mohamed, L. Z., A Comprehensive Review of Silver Nanoparticles (AgNPs): Synthesis Strategies, Toxicity Concerns, Biomedical Applications, AI-Driven Advancements, Challenges, and Future Perspectives, *Arab. J. Sci. Eng.*, 51, 13667-13714(2026). https://doi.org/10.1007/s13369-025-10612-0

Hublikar, L.V., Ganachari, S.V., Patil, V. B., Nandi, S. and Honnad, A., Anticancer potential of biologically synthesized silver nanoparticles using Lantana camara leaf extract, *Prog. Biomater.*, 12, 155–169 (2023). https://doi.org/10.1007/s40204-023-00219-9

Hussain, M., Nafady, A., Sirajuddin Avcı, A., Pehlivan, E., Nisar, J., Sherazi, S., Balouch, A., Shah, M., Almaghrabi, O. and Ul-Haq, M., Biogenic Silver Nanoparticles for Trace Colorimetric Sensing of Enzyme Disrupter Fungicide Vinclozolin, *Nanomater.*, 9, 1604(2019). https://doi.org/10.3390/nano9111604

Iravani, S., Green synthesis of metal nanoparticles using plants. *Green Chem.*, 13(10), 2638–2650 (2011). https://doi.org/10.1039/c1gc15386b

Jabeen, S., Qureshi, R., Munazir, M., Maqsood, M., Munir, M., Shah, S. S. H. and Rahim, B. Z., Application of green synthesized silver nanoparticles in cancer treatment—a critical review, *Mater. Res.*

Exp., 8(9), 092001(2021). https://doi.org/10.1088/2053-1591/ac1de3

Jalilzadeh, M., Asnaashari, S., Alizadeh, A. A., Dastmalchi, S. and Javadzadeh, Y., Synthesis, Physicochemical Properties, and Cytotoxicity of Silver Nitrate Nanoparticles of Achillea filipendulina L. Extract in Lung Cancer Cells, *Pharma. Sci.*, 31(4), 391–402(2025). https://doi.org/10.34172/PS.025.40953

Javid, S. H. and Dilshad, E., Artemisia carvifolia Buch silver nanoparticles downregulate the Rap2A gene in liver cancer, *Sci. Rep.*, 13(1), (2023). https://doi.org/10.1038/s41598-023-48946-0

Joy, A., Satheesan, K. and Paul, A., High-resolution maximum air temperature estimation over India from MODIS data using machine learning, *Remote Sensing Appli. Soc. Environ.*, 37, 101463 (2025). https://doi.org/10.1016/j.rsase.2025.101463

Juvé, V., Cardinal, M. F., Lombardi, A., Crut, A., Maioli, P., Pérez-Juste, J., Liz-Marzán, L. M., Del Fatti, N. and Vallée, F., Size-Dependent Surface Plasmon Resonance Broadening in Nonspherical Nanoparticles: Single Gold Nanorods, *Nano Lett.*, 13(5), 2234–2240(2013). https://doi.org/10.1021/nl400777y

Kanagavalli, U., Sadiq, A. M., Sathishkumar, and Rajeshkumar, S., Plant Assisted Synthesis of Silver Nanoparticles Using *Boerhaavia diffusa* Leaves Extract and Evolution of Antibacterial Activity, *Res. J. Pharm. Technol.*, 9(8), 1064-1068(2016a). https://doi.org/10.5958/0974-360X.2016.00201.8

Kapuscinski, J., DAPI: a DNA-Specific Fluorescent Probe, *Biotech. Histochem.*, 70(5), 220–233 (1995). https://doi.org/10.3109/10520299509108199

Kelly, K. L., Coronado, E., Zhao, L. L. and Schatz, G. C., The Optical Properties of Metal Nanoparticles: The Influence of Size, Shape, and Dielectric Environment, *J. Phys. Chem. B*, 34(16), 668–677(2003). https://doi.org/10.1002/chin.200316243

Khan, M. S., Alomari, A., Tabrez, S., Hassan, I., Wahab, R., Bhat, S. A., Alafaleq, N. O., Altwaijry, N., Shaik, G. M., Zaidi, S. K., Nouh, W., Alokail, M. S. and Ismael, M., Anticancer Potential of Biogenic Silver Nanoparticles: A Mechanistic Study, *Pharm.*, 13(5), 707–707 (2021). https://doi.org/10.3390/pharmaceutics13050707

Kim, S. and Ryu, D., Silver nanoparticle-induced oxidative stress, genotoxicity and apoptosis in cultured cells and animal tissues, *J. Appl. Toxicol.*, 33(2), 78–89(2013). https://doi.org/10.1002/jat.2792

Kodhaiyolii, S. Mohanraj, S. Rengasamy, M. and Pugalenthi, V. Phytofabrication of bimetallic Co–Ni nanoparticles using *Boerhavia diffusa* leaf extract: analysis of phytocompounds and application for simultaneous production of biohydrogen and bioethanol. *Mater. Res. Express*, 6, 095051, (2019). 10.1088/2053-1591/ab2ea8

Kumarasamy, R. V., Natarajan, P. M., Mathivanan, I. Balasubramaniam, M., Suresh, S., Prabhu, D., Raju, K., Mironescu, M. and Mironescu, I. D., Sustainable biogenic synthesis of silver nanoparticles for oral cancer: a comprehensive review, *Front. Nanotechnol.*, 7, (2026).

Lee, J. S., Lytton, J. A. K. R., Hurst, S. J. and Mirkin, C. A., Silver Nanoparticle−Oligonucleotide Conjugates Based on DNA with Triple Cyclic Disulfide Moieties, *Nano Lett.*, 7(7), 2112–2115 (2007). https://doi.org/10.1021/nl071108g

Madhusudanan, M., Green Synthesis of Silver Nanoparticles and their Polymer Composites for Enhanced Antimicrobial and Anticancer Applications, *Res. Port. Denmark*, 183(2024).

Mariano, S., Panzarini, E., Carata, E. and Dini, L., In vitro comparative study of the effects of silver and gold nanoparticles exploitable in the context of photodynamic therapy, *AIP Conf. Proce*., 1990, 020023(2018). https://doi.org/10.1063/1.5047777

Mosmann, T., Rapid colorimetric assay for cellular growth and survival: Application to proliferation and cytotoxicity assays, *J. Immunol. Meth.*, 65, 55–63 (1983).

Mustapha, T., Misni, N., Ithnin, N. R., Daskum, A. M. and Unyah, N. Z., A Review on Plants and Microorganisms Mediated Synthesis of Silver Nanoparticles, Role of Plants Metabolites and Applications, *Int. J. Environ. Res. Pub. Hea.*, 19(2), 674(2022). https://doi.org/10.3390/ijerph19020674

Palle, S., Penchalaneni, J., Lavudi, K., Gaddam, S. A., Kotakadi, V. S. and Challagundala, N., Green Synthesis of Silver Nanoparticles by Leaf Extracts of Boerhavia erecta and Spectral Characterization and Their Antimicrobial, Antioxidant ad Cytotoxic Studies on Ovarian Cancer Cell Lines, *Lett. Appl. Nano. Bio. Sci.*, 9(3), 1165–1176(2020). https://doi.org/10.33263/LIANBS93.11651176

Pandey, P., Lakhanpal, S., Bishoyi, A. K., Jyothi, S. R., Mishra, S., Verma, M., Singh, A. V., Alam, M. W., Rab, S. O., Saeed, M. and Khan, F., Biosynthesis of silver nanoparticles from plant extracts: a comprehensive review focused on anticancer therapy, *Front. Pharmacol.*, 16, 1600347–1600347 (2025). https://doi.org/10.3389/fphar.2025.1600347

Krishnamoorthy, P. K. P., Muthukumaran, S., Maheswaran, A. and Sukumaran, P., Isolation, purification and characterization of boeravinone b from *Boerhaavia diffusa* Linn, *Int. Res. J. Pharm.*, 8, 140–144(2017). https://doi.org/10.7897/2230-8407.0811233

Reena, J. A. and Gayathri, D., Green Synthesis of Silver Nanoparticle using Ethanolic Extract of *Boerhavia diffusa* and it's *in vitro* Antioxidant Activity, *Ind. J. Nutri. Diet.*, 61(4), 441–452(2024). https://doi.org/10.21048/IJND.2024.61.4.32564

Ribble, D., Goldstein, N. B., Norris, D. A. and Shellman, Y. G., A simple technique for quantifying apoptosis in 96-well plates, *BMC Biotechnol.*, 5, 12 (2005). https://doi.org/10.1186/1472-6750-5-12

Roy, A., Plant Derived Silver Nanoparticles and their Therapeutic Applications, *CPB*, 22(14), 1834–1847 (2021). https://doi.org/10.2174/1389201021666201027155708

Sangappa, Y., Latha, S., Asha, S., Sindhu, P., Parushuram, N., Shilpa, M., Byrappa, K. and Narayana, B., Synthesis of anisotropic silver nanoparticles using silk fibroin: characterization and antimicrobial properties, *Mater. Res. Innov.*, 23, 79–85(2019). https://doi.org/10.1080/14328917.2017.1383680

Sangour, M. H., Ali, I. M., Atwan, Z. W. and Al Ali, A. A. A. L. A., Effect of Ag nanoparticles on viability of MCF-7 and Vero cell lines and gene expression of apoptotic genes, *Egypt J. Med. Hum. Genet.*, 22, 9, (2021). https://doi.org/10.1186/s43042-020-00120-1

Singh, A. K., Kushwaha, P. P., Singh, A. and Pandey, A. K., Overcoming cancer drug resistance: insights into Apoptotic pathway modulation by plant-based nanoparticle and natural products, *Front. Oncol.*, 15, (2025). https://doi.org/10.3389/fonc.2025.1677380

Singh, J., Kumar, A., Nayal, A. S., Vikal, S., Shukla, G., Singh, A., Singh, A., Goswami, S., Kumar, A., Gautam, Y. K., Verma, Y., Gaurav, S. S. and Pratap, D., Comprehensive antifungal investigation of green synthesized silver nanoformulation against four agriculturally significant fungi and its cytotoxic applications, *Sci. Rep.*, 14, 5934(2024). https://doi.org/10.1038/s41598-024-56619-9

Soni, D. and Gandhi, D., Toxicity evaluation of silver nanoparticles synthesized from naringin flavonoid on human promyelocytic leukemic cells and human blood cells, *Toxicol. Ind. Hea.*, 40(3), 125–133 (2024). https://doi.org/10.1177/07482337241227244

Stuart, B. Infrared Spectroscopy. In: Wolstenholme, R., Jickells, S., Forbes, S. (Eds.), Analytical Techniques in Forensic Science, Wiley, pp. 145–160. https://doi.org/10.1002/9781119373421.ch7

Takáč, P. Michalková, R. Čižmáriková, M. Bedlovičová, Z. Balážová, Ľ. and Takáčová, G. The Role of Silver Nanoparticles in the Diagnosis and Treatment of Cancer: Are There Any Perspectives for the Future? *Life*, 13(2), 466(2023). https://doi.org/10.3390/life13020466

Todaria, M., Maity, D. and Awasthi, R., Biogenic metallic nanoparticles as game-changers in targeted cancer therapy: recent innovations and prospects, *Future J. Pharma. Sci.*, 10, 25 (2024). https://doi.org/10.1186/s43094-024-00601-9

Tripathi, S., Mahra, S., Sharma, S., Mathew, S. and Sharma, S., Interaction of silver nanoparticles with plants: A focus on the phytotoxicity, underlying mechanism, and alleviation strategies, *Plant Nano Bio.*, 9, 100082 (2024). https://doi.org/10.1016/j.plana.2024.100082

Ullah, M. N., Umer, A., Aadil, M. A., Rehman, F. and Ramzan, N., Plant-based synthesis of silver nanoparticles and their characteristic properties, *Bioinspired, Biomimetic Nanobiomater.*, 6(1), 20–36(2017). https://doi.org/10.1680/jbibn.16.00033

Venkataramana, B., Sankar, S. S., Saikumar, A. and Naidu, B. V. K., Phytochemical Mediated Synthesis of Silver Nanoparticles using Musa paradisiaca Peduncle Latex and Its Photocatalytic and Antimicrobial Activity, *J. Nanosci. Technol.,* 4(5), 503–507(2018). https://doi.org/10.30799/jnst.151.18040511

Vishal, J., Ranjani, S., Ravindranath, K. J. and Hemalatha, S., Synthesis, characterization and evaluation of antioxidant, anticancer and toxicity properties of silver nanoparticles synthesized from Syzygium aromaticum, *Archives Breast Cancer*, 10(3), 291–300(2023). https://doi.org/10.32768/abc.2023103291-300

Wang, M., Zheng, Q., Shen, Q. and Guo, S., The Critical Role of Potassium in Plant Stress Response, *IJMS*, 14(4), 7370–7390(2013). https://doi.org/10.3390/ijms14047370

Yeşilot, Ş. and Dönmez, S., Cytotoxic effect of green synthesized silver nanoparticles with salvia officinalis on MCF-7 human breast cancer cells, *Turkish J. Hea. Sci. Life,* 4(3), 133-139 (2021). https://izlik.org/JA49KG49JB

Zhang, C., Jeong, C. B., Lee, J. S., Wang, D. and Wang, M., Transgenerational Proteome Plasticity in Resilience of a Marine Copepod in Response to Environmentally Relevant Concentrations of Microplastics, *Environ. Sci. Technol.*, 53(14), 8426–8436(2019). https://doi.org/10.1021/acs.est.9b02525